# CSDF-by-SIREN: Learning Signed Distances in the Configuration Space Through Sinusoidal Representation Networks

Christoforos Vlachos<sup>©a</sup> and Konstantinos Moustakas<sup>©b</sup>

Department of Electrical and Computer Engineering, University of Patras, 26504 Rion-Patras, Greece

Keywords: Configuration Space Signed Distance Function (CSDF), Sinusoidal Representation Networks (SIREN), Neu-

ral Implicit Representation, Robot Configuration Space, Signed Distance Function (SDF), Inverse Kinematics.

Signed Distance Functions (SDFs) are used in many fields of research. In robotics, many common tasks, such as motion planning and collision avoidance use distance queries extensively and, as a result, SDFs have been integrated widely in such tasks, fulfilling even the tightest speed requirements. At the same time, the idea of the more natural representation of distances directly in the configuration space (C-space) has been gaining ground, resulting in many interesting publications in the last few years. In this work, we aim to define a C-space Signed Distance Function (CSDF) in a way that parallels other SDF definitions. Additionally, coupled with recent advancements in machine learning and neural representation of implicit functions, we attempt to create a neural approximation of the CSDF in a way that is fast and accurate. To validate our contributions, we construct an experiment environment to test the accuracy of our proposed workflow in an inverse kinematics contact test. Comparing these results to the performance of another published approach to the neural implicit representation of distances in the Configuration Space, we found that our method offers a considerable improvement, reducing the measured errors and increasing the success rate.

#### 1 INTRODUCTION

Abstract:

Among the many fields of robotics, the concept of distance has always played a critical role in the way a robot interprets and interacts with its environment. Whether it is used as a measurement of separation between points, obstacles, or a robot's end effector and its target location, it provides valuable information for many common tasks.

Specifically regarding the field of robotics, Signed Distance Functions (SDFs) have been studied extensively and are well-incorporated in many manipulation, control, and optimization tasks. A lot of operations in robotics often need to transition between representing quantities in task-space or configuration-space (often abbreviated to "C-space"). As such, representations of the SDF in C-space by transforming the task-space are often used.

A different approach which, among many advantages, fits well in multiple common robotics workflows, is the definition of a distance function directly in the C-space. This function may be used instead of

the transformed task-space SDF in order to intuitively and robustly represent the angular distance between a robotic arm and some point in the C-space.

The learning of implicit functions has been a focal point in many publications during the last years, exhibiting remarkable results (Park et al., 2019; Mildenhall et al., 2020; Mescheder et al., 2019). Naturally, SDFs have played a major role in this opportune occasion, with many researchers opting to use this form of implicit representation as an alternative to explicit mesh representation, featuring important advantages (Gropp et al., 2020; Hao et al., 2020; Yariv et al., 2021). And while neural networks for learning SDFs in the convenience of readily defined Euclidean spaces have been well investigated, learning such functions directly in a robot's C-space is a relatively immature and largely uncharted subject.

Code and pretrained models of this work may be found in the following repository: https://github.com/ChristoforosVlachos/CSDF.git

<sup>&</sup>lt;sup>a</sup> https://orcid.org/0000-0003-2863-7823

b https://orcid.org/0000-0001-7617-227X

#### 2 RELATED WORK

#### 2.1 Implicit Representation

Although a very traditional technique, the explicit representation of surfaces has been questioned numerous times as a choice for a lot of applications. This is especially true when we are interested in representing continuous surfaces where a discretization of space may prove detrimental to the task. As such, level set methods surfaced very early on (Osher and Fedkiw, 2003; Breen and Whitaker, 1999; Bloomenthal and Bajaj, 1997) to apply implicit functions to the common task of surface representation in fluid dynamics, modeling, as well as motion planning and robotics jobs.

#### 2.2 Neural Implicit Representation

Amid neural methods becoming mainstream, implicit representations turned to leverage the neural research that was quickly becoming the status quo. Thus, many researchers were now using deep learning in order to accurately and efficiently approximate continuous implicit functions. As far as radiance fields go, *NeRF* sa introduced by Mildenhall et al. (Mildenhall et al., 2020) went on to become complete game-changers, whereas Mescheder et al. promoted occupancy fields for 3D shape representation (Mescheder et al., 2019).

Signed Distance Fields and Signed Distance Functions played a major role in neural implicit representation. The first major work to introduce neural SDFs for implicitly representing 3D shapes was Park et al.'s *DeepSDF* in 2019 (Park et al., 2019), competing with Mescheder et al.'s *Occupancy Networks* (Mescheder et al., 2019). Other works soon followed to improve upon those initial concepts (Gropp et al., 2020; Ortiz et al., 2022), with Sitzmann et al.'s noteworthy research in the use of periodic activation functions in place of other nonlinearities to very accurately represent continuous functions (Sitzmann et al., 2020). Those networks were nicknamed SIRENS (Sinusoidal Representation Networks) and provide the technical basis of our proposed workflow.

# 2.3 Signed Distance Functions in Robotics

The concept of Signed Distance Functions was brought over to robotics, as it seemed a natural fit for common tasks, such as collision detection/avoidance and motion planning. Ratliff et al. (Ratliff et al., 2015) were among the first to use the notion of a distance function that is negative inside an object and positive

outside to encode obstacles for motion planning in 2015. Liu et al. (Liu et al., 2022) later extended SDF-based representations with deep learning, a concept which led Ortiz et al. (Ortiz et al., 2022) to develop *iSDF*, a real-time neural SDF approach, enabling the use of SDFs in dynamically changing environments.

### 2.4 C-Space Distance Functions

While SDFs usually operate in the robot's workspace, an extension to this notion has been presented in the literature that aims to express distance functions directly in the C-space, where robot motion is naturally defined. Recent work by Li et al. (Li et al., 2024a) formalized the (unsigned) Configuration space Distance Field (CDF) and used them in various applications such as inverse kinematics and motion planning. Doing the required computations analytically though is quite expensive.

To combat this problem, Koptev et al. (Koptev et al., 2023) had earlier focused and experimented on a neural representation of signed distance functions for articulated robots. Inspired by this work, Li et al. (Li et al., 2024a) also propose a neural extension of their work, named the "neural-CDF" (since our work also focuses on a neural approach, we will often omit that part and refer to it simply as "CDF").

# 3 MOTIVATION – CONTRIBUTIONS

In the rest of this paper, we will cover a mathematical definition of a Configuration Space Signed Distance Function, a complete methodology for obtaining a robust neural approximation of such a function, as well as rigorous validation and comparison in standard robotics workflows. Our work aims to fill existing gaps in research, hoping to serve this innovative field of research.

Concisely, our contribution focuses on the following items:

- formalize the definition of a Configuration Space Signed Distance Function (CSDF) as a mathematical quantity and fit it inside the distance functions spectrum.
- define a methodology to enable the creation of a neural structure to obtain the CSDF quickly and accurately. Similar structures have yet to be deployed and examined in such high dimensional environments.
- improve upon existing relevant solutions in terms of speed, memory requirements, and fidelity.

#### 4 METHODS

#### 4.1 Background

A distance function is usually defined as a scalar function f(x) that represents the (minimum) distance between point x and a second object. This definition holds, even when  $x \in \mathbb{R}^n$  and n > 3.

In the case of the SDF,  $\phi(x)$ , it is commonly expressed as:

$$\phi(x) = \begin{cases} 0 & , & x \in \partial \Omega \\ d(x), & x \in \Omega^+ \\ -d(x), & x \in \Omega^- \end{cases}$$
 (1)

where  $\Omega \subseteq \mathbb{R}^n$  and  $\partial \Omega$  represents an airtight boundary iso-surface splitting  $\Omega$  into  $\Omega^+$  (the part of the space outside the iso-surface) and  $\Omega^-$  (the part of the space enclosed by the iso-surface). d(x) then represents the distance between x and the nearest point of  $\partial \Omega$ . The negative sign is given to  $\Omega^-$  by convention.

While the concept of the SDF is often seen and used in a multitude of manners and in various problems of robotics, a new form of distance functions, the C-space Distance Functions, is gaining ground. Even though our human intuition processes perfectly Euclidean robot workspaces well, to a robot the (usually non-Euclidean) C-space is a much more intuitive environment where its operations can be defined easily, even naturally. To this extent, the collection of distance functions may be broadened to contain

$$\phi_c(x) = \begin{cases} 0 & , & x \in \partial \Omega_c \\ d_c(x), & x \in \Omega_c^+ \\ -d_c(x), & x \in \Omega_c^- \end{cases}$$
 (2)

where  $d_c$  represents distance in C-space, which may be geodesic, angular, or a combination of the two. Here  $\partial\Omega_c$  is, again, a boundary surface splitting  $\Omega_c$  into an outside region  $\Omega_c^+$  and an inside region  $\Omega_c^-$ .  $\Omega_c$  may be chosen to be a subset of the C-space or it may not; this detail is heavily influenced by the conditions of the relevant task.

It should be emphasized that Equation 2 is no different than Equation 1. It is only a specific case expressed formulaically for clarity. This is in contrast to simply applying a transformation to an existing SDF defined in the robot's workspace to be expressed in the domain of its C-space, as is very well demonstrated in (Li et al., 2024a). Moreover, the CSDF is similarly distinct from its unsigned counterpart introduced in the same work in that a CSDF is not merely a sub-category of SDF – it is an SDF, defined in a space where distance is measured geodesically.

One more point of note is that, when talking in terms of the CSDF (or, likewise, the SDF) of a robot, this function is modified as the robot navigates its workspace. Therefore, we should rewrite the CSDF in the form  $\phi_c(p,q)$ , expressing it relative to both the query point  $p \in \mathbb{R}^n$  and the robot's current configuration  $q \in \mathbb{R}^m$ , with n representing the dimensionality of the workspace (normally, 2 or 3) and m being the number of Degrees-of-Freedom of the robot in use.

With our proposed approach, the neural representation of the CSDF  $\phi_c(p,q)$  is equivalent to the representation of the distance function  $\phi_c(x)$ , when x = [p,q] and  $x \in \mathbb{R}^{(n+m)}$  (in other words, here we set  $\Omega_c \subseteq \mathbb{R}^{(n+m)}$ ). This approach exposes the problem of the CSDF representation to be completely analogous to that of representing any SDF of possibly high dimensionality n+m- and it should be treated as such.

#### 4.2 Neural Implicit Representation

We are interested in obtaining an approximation of  $\phi_c(p,q)$ , which we call  $\hat{\phi}_c(p,q)$ , by neural network. There are many possibilities for the choice of architecture that have appeared in literature (Park et al., 2019; Gropp et al., 2020), each with their own advantages, prevalent features, and areas of expertise. One specific architecture, namely the Sinusoidal Representation Network (SIREN) (Sitzmann et al., 2020), has demonstrated great results in the representation of continuous signals (including SDFs) (Vlachos and Moustakas, 2024) and appears very well suited for the task at hand.

SIRENS, to be concise, are comprised of a few fully connected NN layers. They differ from usual MLPs in that they employ sinusoidal activation functions instead of opting for the usual nonlinearities (ReLU, tanh, etc.). While their usefulness has been demonstrated in tasks of generally low dimensionality, they are yet to be tested in high dimensionality problems, as is the approximation of the CSDF.

We constructed a SIREN consisting of 1 input, 1 output, and 3 hidden layers. This distribution of layers is common in literature and usually obtained the best results in our own testing. The input layer consists of (n+m) neurons to input the query point  $p \in \mathbb{R}^n$  and current robot configuration  $q \in \mathbb{R}^m$ , while the output layer contains only a single neuron to output the value of the predicted CSDF,  $\widehat{\phi}_c(p,q)$ . Different amounts of neurons for the hidden layers were investigated. Two variants are showcased here, one with 512 neurons per hidden layer, and a lighter one, with 256 neurons per hidden layer. The architecture of our proposed SIREN solution can be examined in Figure 1.

To aid the SIREN in its difficult task of approxi-

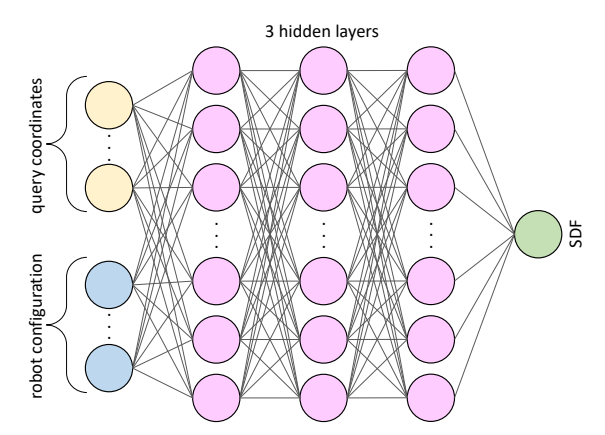


Figure 1: The architecture of our proposed SIREN for a quality approximate representation of the C-Space Signed Distance Function (CSDF).

mating the CSDF, an appropriate loss function must be deployed. Based on previously published literature of similar tasks (Li et al., 2024a; Sitzmann et al., 2020), we constructed the following loss function:

$$\mathcal{L}_{csdf} = w_1 \int_{\Omega_c} \||\nabla_q \widehat{\phi}_c(p, q)| - 1\| dx$$

$$+ w_2 \int_{\Omega_c} (1 - \langle \nabla_q \widehat{\phi}_c(p, q), \nabla_q \phi_c(p, q) \rangle) dx$$

$$+ w_3 \int_{\Omega_c} |\widehat{\phi}_c(p, q) - \phi_c(p, q)| dx$$

$$+ w_4 \int_{\Omega_c} \|\nabla_q^2 \widehat{\phi}_c(p, q)\|^2 dx$$

$$(3)$$

In Equation 3, the first integral enforces the, so called, eikonal equation on the entire space  $\Omega_c$ . Being a distance function, for the CSDF it is fundamental that  $\|\nabla_x \phi_c(x)\| = 1$  almost everywhere (except for a few degenerate points (Osher and Fedkiw, 2003)). The second integral is a classic cosine similarity loss which ensures that the predicted CSDF has a similar direction with the ground-truth CSDF.

The third integral is a direct comparison of the predicted function to the ground-truth values. There is a key distinction between this term and the one suggested by (Li et al., 2024a): instead of minimizing distance errors using the L2 norm, we use the L1 norm (absolute difference). This subtle change leads to improved accuracy and stability, preventing excessive error penalization and ensuring smoother convergence. In high-dimensional C-space representations, our approach mitigates the disproportionate influence of large errors seen with L2-based losses, resulting in a more precise CSDF approximation.

A fourth integral may be optionally added in order to curb the second-order derivatives of the predicted function, maintaining smooth changes. We identified this term as a viable regularization option by our own ablation experiments and observed a measurable improvement when using it.

Studying the proposed loss function, since the second and third integral terms require knowledge of the ground truth CSDF,  $\phi_c(p,q)$ , it is immediately evident that the calculation of the ground truth CSDF, at least for select samples to be used as input data will be unavoidable. For lower dimensionality distance functions, we might have evaded using different loss terms that do not require knowledge of the groundtruth CSDF, leveraging insightful heuristics, similar to (Sitzmann et al., 2020). Here, such a simplification is likely not possible. In the following experiments, the weights of the individual loss terms were set to  $w_1 = 0.01$ ,  $w_2 = 0.1$ ,  $w_3 = 5.0$ , and  $w_4 = 0.01$ , as per the existing literature (Li et al., 2024a). These ensure a good match with the available ground truth data, while also using less enforced terms to assist in regularization.

#### **5 EXPERIMENTS**

To assess the performance of our proposed solution, both in terms of accuracy and speed, we simulated an environment where a single 7-DoF Franka Emika robotic arm was tasked to make contact with one specific point in the robot's 3D task space.

As ground truth data, we followed the dataset generation instructions in (Li et al., 2024a). They were obtained by creating a sampling grid of dimensions  $20 \times 20 \times 20$  from the robot's workspace and, through optimization techniques, finding the configurations q' that satisfy  $\phi(p,q')=0$  for each point p in the grid.  $\phi(p,q)$  represents the SDF model of the robot i.e., a function that is able to represent the signed distance of point p to the robot in configuration q. This kind of problem has been tackled before (Koptev et al., 2023; Liu et al., 2022). We made use of the SDF model published in (Li et al., 2024b) in order to compete with neural-CDF (Li et al., 2024a) in a fair manner.

As far as the implementation of the contact task is concerned, we adopt the following process. By calculating  $\widehat{\phi}_c(p,q_{i-1})=d_c$  at each iteration i, we determine the appropriate movement as:

$$\Delta q_i = -\widehat{\phi}_c(p, q_{i-1}) \times \nabla_q \widehat{\phi}_c(p, q_{i-1}) \tag{4}$$

and, consequently,  $q_i = q_{i-1} + \Delta q_i$ . The derivative is calculated by auto-differentiation.

If the solution works well, it is expected that  $q_i$  would converge to a configuration q' with the property that  $\phi(p,q') = 0$ . Therefore, after each iteration step,  $\phi(p,q_i)$  is calculated and this function's magnitude is

regarded as error. For increased precision in testing, we repeat this test for 1000 pairs of points p and initial configurations  $q_0$ . As metrics, we report the mean average error (MAE) and the root mean square error (RMSE). The success rate (SR) is also reported as another metric and is defined as the percentage of configurations  $q_i$  that were sufficiently close to the target point p, less than 3 cm away.

#### 6 RESULTS

Li et al. (Li et al., 2024a) have recently worked on C-Space Distance Fields, presenting a similar method for obtaining a neural representation of the (unsigned) C-Space Distance Function using a simple MLP enhanced by positional encoding. Although our approach targets a similar representation, our individual methods differ significantly in many important details. Thus, we consider this a suitable method to compare our solution to, highlighting the value those details carry.

Our proposed SIREN network consists of 3 hidden layers of 512 neurons per layer. On the input side, the 3 cartesian coordinates of the query point are passed to the network, along with the 7 joint angles of the robotic arm (matching the 7 Degrees of Freedom of the Franka Emika), giving us an input dimension of 3 + 7 = 10.

We are also proposing and testing a lighter version of the above SIREN ("SIREN light"), one with only 256 neurons per hidden layer. This is done in order to push the SIREN architecture to its limit and assess its potential.

Each network was trained for  $50\,000$  epochs on an AWS "g5.xlarge" instance featuring a single NVidia A10G Tensor Core GPU with 24 GB of VRAM and 4 vCPUs on a system with 16 GB of RAM. On each epoch, 20 000 points were sampled from the dataset, along with 100 configurations per query point, totaling a batch size of  $20\,000 \times 100$ .

After training, each network was tested on the contact experiment. For each test, the number of iterations the network was allowed in order to manage contact was kept fixed. The results of these experiments may be found on Table 1. Reported are means and variances of the relevant metrics obtained by repeating each test 100 times. A few sample iterations may be seen rendered in Figure 2.

Looking at Table 1, we notice that the CDF approach (MLP with positional encoding) gives a poor success rate after the first iteration, and significantly better results afterwards, reaching its peak performance after 5 iterations. In contrast, using our pro-



Figure 2: Four rendered frames from the contact experiments. In each run, the Franka Emika robot is tasked with making contact with a specific point inside its task space (a small, colored sphere is used to represent said point) but has only a set amount of C-space moves to get there. It is observed and validated that contact is apparently achieved.

posed SIREN, we achieve adequate results after the first iteration already. By the second iteration, we have honed the success rate to 93.8%, 2% better than CDF ever managed. At the third iteration, the success rate rises to its peak: 95.4%. Even our proposed "SIREN light" variant hits consistently lower errors and a higher success rate than CDF.

SIRENS are known for converging very fast and with little data to an accurate solution. In order to let our approach truly demonstrate its potential, we chose to repeat the experiment, this time training each network on a way smaller batch size of 10 points  $\times$  100 configurations, for 50 000 epochs too. Then, a repeat of the contact task was performed, providing the results of Table 2.

This time, we notice that the CDF method fails to produce decent results, struggling to reach a 78% success rate even after 5 iterations. On the other hand, our proposed SIREN for approximating the CSDF achieves great results after only 2 iterations. With further adjustment iterations, the success rate reaches 90.7%. The "SIREN light" follows the same story, trailing closely behind "SIREN" and managing a plateau of 90% success rate.

Another dimension of the problem, which we have yet to discuss is the offline training time of each representation, as well as the number of trainable parameters, which directly influences the memory requirements. For the experiments that were performed, a collection of these measurements can be seen on Table 3. It should be noted that all the improvements that were achieved by our method, were attained with less training time on a representation utilizing fewer parameters. It is also worth pointing out that our testing suggested that the large training time of the full SIREN

Table 1: Results of the contact experiment. Calculation of the C-space distances and gradients is performed by CDF (Li et al., 2024a), our SIREN-based approach for CSDF, and by a lighter version of the same network. All networks were trained on a batch size of  $20000 \times 100$  for 50000 epochs. Results after 1, 2, 3, 4, 5, or 10 iterations are displayed. For Mean Average Error (MAE) and Root Mean Squared Error (RMSE), lower is better. For Success Rate (SR), higher is better.

Table 2: Results of the contact experiment, similar to Table 1. All networks were trained on a batch size of  $10 \times 100$  for 50000 epochs.  $\left| \begin{array}{c|c} \leftarrow & 5 & 5 & 5 & 5 & 5 \\ \hline & 2 & 6 & 6 & 5 & 5 \\ \hline & 2 & 1 & 2 & 2 & 5 \\ \hline \end{array} \right|$ 

Results after 1, 2, 3, 4, 5, or 10 iterations for Mean Average Error (MAE) and Root Error (RMSE), lower is better. For Success or is better.					SR (%	50.4±	$83.5\pm$	$88.7 \pm$	$90.0 \pm$	$89.3 \pm$	$88.4 \pm$					
SIREN light	SR (%) ↑	E 8.6 ∓ 9.29	$93.1 \pm 4.8$	$95.0 \pm 5.3$	$94.6 \pm 7.2$	$93.5 \pm 7.7$	$93.1 \pm 8.4$		SIREN light	RMSE (cm) $\downarrow$	$11.73 \pm 4.49$	$4.25\pm1.81$	$2.58\pm1.04$	$2.17 \pm 0.93$	$2.19 \pm 1.01$	$2.23 \pm 1.20$
	RMSE (cm) $\downarrow$	$9.46 \pm 3.82$	$3.03 \pm 1.37$	$1.79 \pm 0.71$	$1.66\pm0.71$	$1.72 \pm 0.76$	$1.81\pm1.00$			MAE (cm) ↓ R			$1.58 \pm 0.53$			$.57 \pm 0.72$
	MAE (cm) $\downarrow$	$5.03 \pm 2.06$	$1.46\pm0.47$	$1.21 \pm 0.37$	$1.22 \pm 0.41$	$1.27 \pm 0.44$	$1.34\pm0.55$			SR (%) ↑ M.		$85.9\pm 9.3$ 2.				9.3
	SR (%) ↑	$70.2 \pm 10.3$					93.4 ± 8.0									1.15 90.4±
SIREN	RMSE (cm) $\downarrow$	$8.91 \pm 3.75$ 7				$609.0 \pm 99.0$	$.75\pm0.78$	EPF	SIREN	RMSE (cm) ↓	$11.00 \pm 4.24$	$3.79 \pm 1.62$	2.32 士	$2.07 \pm 0$	$2.02 \pm 0$	2.09 =
				_			_	TECHNOLOGY	F	MAE (cm) ↓	$6.69 \pm 2.75$	$.94 \pm 0.76$	$.47 \pm 0.57$	$.42 \pm 0.58$	$.41 \pm 0.49$	$.46 \pm 0.64$
	MAE (cm) ↓	$4.61 \pm 1.94$	$1.38 \pm 0.43$	$1.17 \pm 0$	$1.20 \pm 0$	$1.24 \pm 0.41$	$1.33 \pm 0.49$			(%) ↑ W	12.2		_	1	14.0 1	14.8
	SR (%) ↑	$59.8\pm12.1$		$.2 \pm 8.6$			.2± 8.9			SR (%	39.5±	$69.8 \pm 12.4$	$77.8 \pm 13.2$	$77.8\pm$	$77.9 \pm 14.0$	75.5±
CDF	RMSE (cm) ↓ S	$8.62 \pm 3.12$ 59							CDF	RMSE (cm) ↓	$11.48 \pm 3.93$	$4.79\pm1.66$	$3.38 \pm 1.36$	$3.20 \pm 1.26$	$3.20 \pm 1.43$	$3.29\pm1.43$
	MAE (cm) ↓ R					$1.36\pm0.53$				MAE (cm) $\downarrow$	$7.86 \pm 2.73$	$2.98\pm1.07$	$2.23 \pm 0.92$	$2.18 \pm 0.86$	$2.19 \pm 0.93$	$2.31\pm1.01$
Projection	Iterations	_	2	В	4	5	10		Projection	Iterations	1	2	8	4	S	10

Batch Size	Approach	Training Time	Trainable Parameters
20000	CDF	5:37:13	737 409
×	SIREN	5:53:40	531 457
100	SIREN light	4:17:30	134 657
10	CDF	2:15:44	737 409
×	SIREN	1:33:33	531 457
100	SIREN light	1:34:14	134 657

Table 3: Training time for 50000 epochs and number of trainable parameters for the neural-CDF network (Li et al., 2024a), for our SIREN-based approach, and for the lighter version of the same network.

approach at a large batch size was likely caused by a memory fragmentation issue in our system. Furthermore, no decrease in training time is observed using the light variant over the full SIREN variant for the smaller batch size, as for a batch size this small the training operations take severely less time and hardware overheads come heavily into play. Although this means that training may take less time on different systems, the fact that such issues can occur should be kept in mind when implementing any of the discussed methods.

Ultimately, it is important to note that, evidently, the "light" variant of our proposed workflow is likely the most desirable middle ground in terms of accuracy, training time, and memory requirements. In order to squeeze out that last bit of a accuracy, one may use our full-sized SIREN workflow. Either way, our proposed solutions far outperform the alternatives.

## 7 CONCLUSION AND FUTURE WORK

We have clearly and robustly defined the C-space Signed Distance Function (CSDF) as a form of a SDF. We have posed the problem of representing an implicit function, such as the CSDF, utilizing recent advancements in neural implicit representation and work on C-space Distance Functions. We have proposed a methodology for creating a neural approximation and implemented two variations of our proposed method. We have set up an experiment to validate and compare our method to another recently published approach tackling the same problem and found that our method of representing the CSDF easily outperforms the alternative.

In the future we aim to refine our approach with more rigorous experimentation across many scenarios and between different methods. Our very promising results indicate that, provided a careful approach is taken, this method can offer robust solutions to many problems in the general field of robotics, such as motion planning and inverse kinematics. Specifically, details such as the loss function should be investigated further, as, while most of the literature agrees on the fundamental parts, some details are left to be settled.

#### ACKNOWLEDGMENTS

The research project is implemented in the framework of H.F.R.I. call "Basic research Financing (Horizontal support of all Sciences)" under the National Recovery and Resilience Plan "Greece 2.0" funded by the European Union – NextGenerationEU (H.F.R.I. Project Number: 16469).

#### REFERENCES

Bloomenthal, J. and Bajaj, C. (1997). *Introduction to implicit surfaces*. Morgan Kaufmann.

Breen, D. E. and Whitaker, R. T. (1999). A level-set approach for the metamorphosis of solid models. In *ACM SIGGRAPH 99 Conference abstracts and applications*, SIGGRAPH99, page 228. ACM.

Gropp, A., Yariv, L., Haim, N., Atzmon, M., and Lipman, Y. (2020). Implicit geometric regularization for learning shapes. In 37th International Conference on Machine Learning, ICML 2020, pages 3747–3757.

Hao, Z., Averbuch-Elor, H., Snavely, N., and Belongie, S. (2020). Dualsdf: Semantic shape manipulation using a two-level representation. In Proceedings of the IEEE/CVF Conference on Computer Vision and Pattern Recognition.

Koptev, M., Figueroa, N., and Billard, A. (2023). Neural joint space implicit signed distance functions for reactive robot manipulator control. *IEEE Robotics and Automation Letters*, 8(2):480–487.

Li, Y., Chi, X., Razmjoo, A., and Calinon, S. (2024a). Configuration space distance fields for manipulation planning. In *Robotics: Science and Systems XX*, RSS2024. Robotics: Science and Systems Foundation.

- Li, Y., Zhang, Y., Razmjoo, A., and Calinon, S. (2024b). Representing robot geometry as distance fields: Applications to whole-body manipulation. In 2024 IEEE International Conference on Robotics and Automation (ICRA), page 15351–15357. IEEE.
- Liu, P., Zhang, K., Tateo, D., Jauhri, S., Peters, J., and Chalvatzaki, G. (2022). Regularized deep signed distance fields for reactive motion generation. In 2022 IEEE/RSJ International Conference on Intelligent Robots and Systems (IROS). IEEE.
- Mescheder, L., Oechsle, M., Niemeyer, M., Nowozin, S., and Geiger, A. (2019). Occupancy networks: Learning 3d reconstruction in function space. In 2019 IEEE/CVF Conference on Computer Vision and Pattern Recognition (CVPR). IEEE.
- Mildenhall, B., Srinivasan, P. P., Tancik, M., Barron, J. T., Ramamoorthi, R., and Ng, R. (2020). NeRF: Representing Scenes as Neural Radiance Fields for View Synthesis, page 405–421. Springer International Publishing.
- Ortiz, J., Clegg, A., Dong, J., Sucar, E., Novotny, D., Zollhoefer, M., and Mukadam, M. (2022). isdf: Realtime neural signed distance fields for robot perception. In *Robotics: Science and Systems XVIII*, RSS2022. Robotics: Science and Systems Foundation.
- Osher, S. and Fedkiw, R. (2003). Level Set Methods and Dynamic Implicit Surfaces. Springer New York.
- Park, J. J., Florence, P., Straub, J., Newcombe, R., and Lovegrove, S. (2019). Deepsdf: Learning continuous signed distance functions for shape representation. In 2019 IEEE/CVF Conference on Computer Vision and Pattern Recognition (CVPR), page 165–174. IEEE.
- Ratliff, N., Toussaint, M., and Schaal, S. (2015). Understanding the geometry of workspace obstacles in motion optimization. In 2015 IEEE International Conference on Robotics and Automation (ICRA), page 4202–4209. IEEE.
- Sitzmann, V., Martel, J., Bergman, A., Lindell, D., and Wetzstein, G. (2020). Implicit neural representations with periodic activation functions. *Advances in neural information processing systems*, 33:7462–7473.
- Vlachos, C. and Moustakas, K. (2024). High-fidelity haptic rendering through implicit neural force representation. In *International Conference on Human Haptic*

- Sensing and Touch Enabled Computer Applications, pages 493–506. Springer.
- Yariv, L., Gu, J., Kasten, Y., and Lipman, Y. (2021). Volume rendering of neural implicit surfaces. Advances in Neural Information Processing Systems, 34:4805–4815.

#### **APPENDIX**

During the initial stages of the presented research, a debate in the literature between signed and unsigned distance functions and their advantages, made us wonder whether choosing a signed representation was the better option. While a signed representation was more intuitive to us and we felt that the continuous derivatives was a very attractive feature, unsigned CDFs had been successfully used already. After careful testing, the signed representation appeared as a more robust and stable option for our use cases. It is worth mentioning that under certain circumstances using an unsigned representation might be desirable, if one is willing to sacrifice stability for marginally higher peaks. For the sake of completeness, results for an unsigned C-space Distance Function represented using the same SIRENs are included in Table 4 for the batch size of  $20000 \times 100$  and Table 5 for the batch size of  $10 \times 100$ . These may be directly compared to the results of Table 1 and Table 2, respectively. Additionally, Table 6 serves as an expansion to Table 3 that includes training time for the unsigned cases.

Table 4: Additional results of the contact experiment. Calculation of the C-space distances and gradients is performed by an unsigned variant of our SIREN-based approach, and by a lighter version of the same network. Both networks were trained on a batch size of  $20000 \times 100$  for 50000 epochs. Results after 1, 2, 3, 4, 5, or 10 iterations are displayed. For Mean Average Error (MAE) and Root Mean Squared Error (RMSE), lower is better. For Success Rate (SR), higher is better.

Projection	S	SIREN (unsigned)		SIREN light (unsigned)			
Iterations	MAE (cm) ↓	RMSE (cm) ↓	SR (%) ↑	MAE (cm) ↓	RMSE (cm) ↓	SR (%) ↑	
1	$4.58 \pm 1.80$	$8.97 \pm 3.49$	$70.5 \pm 9.7$	$4.94 \pm 1.93$	$9.25 \pm 3.64$	$67.5 \pm 10.0$	
2	$1.37 \pm 0.46$	$2.78\pm1.19$	$93.9 \pm 6.3$	$1.46 \pm 0.45$	$2.99 \pm 1.26$	$93.0 \pm 5.8$	
3	$1.15 \pm 0.34$	$1.68 \pm 0.63$	$95.6 \pm 4.6$	$1.20 \pm 0.35$	$1.75 \pm 0.65$	$95.3 \pm 5.5$	
4	$1.23 \pm 0.41$	$1.65 \pm 0.66$	$94.6 \pm 6.9$	$1.22 \pm 0.37$	$1.63 \pm 0.60$	$94.5 \pm 5.8$	
5	$1.27 \pm 0.45$	$1.71 \pm 0.75$	$93.9 \pm 7.8$	$1.24 \pm 0.40$	$1.65 \pm 0.59$	$93.8 \pm 6.6$	
10	$1.37 \pm 0.54$	$1.86 \pm 0.91$	$92.8 \pm 8.1$	$1.34 \pm 0.52$	$1.75 \pm 0.78$	$92.8 \pm 9.2$	

Table 5: Additional results of the contact experiment, similar to Table 4. Both networks were trained on a batch size of  $10 \times 100$  for 50000 epochs.

Projection	,	SIREN (unsigned)		SIREN light (unsigned)			
Iterations	MAE (cm) ↓	RMSE (cm) ↓	SR (%) ↑	MAE (cm) ↓	RMSE (cm) ↓	SR (%) ↑	
1	$6.76 \pm 2.62$	$11.11 \pm 4.12$	$52.8 \pm 12.2$	$7.20 \pm 2.97$	$11.64 \pm 4.46$	$51.5 \pm 13.1$	
2	$1.87 \pm 0.73$	$3.58 \pm 1.56$	$86.5 \pm 8.8$	$2.05 \pm 0.84$	$3.93 \pm 1.77$	$84.7 \pm 9.4$	
3	$1.45 \pm 0.59$	$2.26\pm1.00$	$90.5 \pm 8.1$	$1.58 \pm 0.64$	$2.51\pm1.10$	$88.5 \pm 9.4$	
4	$1.39 \pm 0.48$	$1.98 \pm 0.77$	$91.2 \pm 7.6$	$1.49 \pm 0.53$	$2.17\pm0.94$	$89.4 \pm 8.4$	
5	$1.40 \pm 0.54$	$1.99 \pm 0.92$	$91.0 \pm 8.2$	$1.54 \pm 0.62$	$2.23\pm1.04$	$88.8 \pm 9.4$	
10	$1.46\pm0.55$	$2.09 \pm 1.07$	$90.0 \pm 8.9$	$1.65 \pm 0.84$	$2.36\pm1.36$	$87.4 \pm 11.9$	

Table 6: Expanded form of Table 3 to include an unsigned variant of our SIREN-based approach and a lighter version of the same network. Training time is measured for 50000 epochs.

Batch Size	Approach	Training Time	Trainable Parameters	
20000	CDF	5:37:13	737 409	
20000	SIREN	SIREN 5:53:40 531 457		
×	SIREN (unsigned)	5:41:46	331 137	
100	SIREN light 4:17:30 134 657			
100	SIREN light (unsigned)	4:09:08	10.1 007	
10	CDF	2:15:44	737 409	
10	SIREN	1:33:33	531 457	
×	SIREN (unsigned)	1:32:05	331 437	
100	SIREN light SIREN light (unsigned)	1:34:14 1:32:52	134 657	